

Background-signal Parameterization in In Vivo MR Spectroscopy

Y. Coenradie¹, R. de Beer¹, D. van Ormondt¹,
H. Ratiney², S. Cavassila², D. Graveron-Demilly²,

¹ Applied Physics, Delft University of Technology, P.O. Box 5046, 2600 GA Delft, The Netherlands

Phone: +31 15 2786070 E-mail: ormo@si.tn.tudelft.nl

² Lab RMN, CNRS UMR 5012, Université Claude Bernard Lyon I-CPE, France

Phone: +33 472 431049 E-mail: graveron@univ-lyon1.fr

Abstract—This study concerns parameterization and subsequent subtraction of the fast decaying signals of macromolecules from *in vivo* MRS signals of tissue metabolites of interest. The parameterization is done with a State Space approach (HSVD) based on singular value decomposition. The method is tested with a simulated non-exponentially damped macromolecule signal and an exponentially damped metabolite signal, and is compared with mere omission of initial samples. Exact analytic expressions of the macromolecule signal are derived in both the time domain and the frequency domain.

Keywords— SVD, State Space, MRS, macromolecules, metabolites

I. INTRODUCTION

A. Magnetic Resonance Information

Non-invasive *in vivo* detection and quantitation of tissue metabolites plays an increasingly important role in medicine. A promising technique for this task is Magnetic Resonance Spectroscopy (MRS) [1]. However, the signal-to-noise ratio (SNR) of a clinical MRS signal is often low which in turn demands the utmost from the quantitation process. The final stage of this quantitation consists of nonlinear least-squares fitting of an appropriate model function [2] to the MRS signal [3].

Until today, a physical model function capable of describing all details of an *in vivo* MRS signal is not available. Rather, the capabilities of MRS scanners improve unabated and ever more details can be detected. In order to cope, the MRS-modelling community needs to continually update its knowledge of scanners. Another aspect is the need to reduce the measurement time which hampers improvement of the SNR. Ultimately, the best response to these aspects is to invoke as much prior knowledge as one can get about tissue properties, tissue metabolites and MRS-signals emanating from them [4,5]. The ensuing precision of the quantitation can be obtained from the Cramér-Rao lower bounds (CRB's) [2, 6–8].

The present paper concerns a way to handle that part of the MRS signal for which one presently has no model function. The next paragraph provides some information about this problem category.

The (spectral) MRS-frequency of a nucleus depends on the spatial orientation of its host molecule in the living tissue. The faster the host molecule tumbles in its surroundings, the more the orientation-dependent contribution to the MRS-frequency is averaged out. Big molecules are less mobile than small ones. They are constrained to certain orientations. These orientations are randomly distributed over the tissue. It follows that an ensemble of large, less mobile, molecules in living tissue contributes a broad MRS-spectrum – also referred to as ‘background’ – that usually overlaps with the wanted spectrum of mobile tissue metabolites. Knowledge to properly model this mechanism is still incomplete. This is the heart of the problem.

B. Existing Approaches

Pending comprehensive physical modelling of the mentioned motion effects, alternative methods are being devised for coping with the less mobile molecules, which are also indicated by ‘macromolecules’. See, *e.g.*, [9–11] and references therein. Stanley and Pettegrew [9] addressed the problem in the time domain which, in the case of MRS, equals the measurement domain. They exploited the fact that in the time domain, broad spectral features such as mentioned above are strongly damped sinusoids [12]: The less mobile a molecule, the quicker its time-domain signal ‘decays into the measurement noise’. As a consequence, mere omission of a sufficient number of initial samples in the time-domain model fit could solve their problem in a natural fashion. Seeger *et al.* [10] separated the contributions of mobile and less mobile molecules during the actual measurement process, using a Magnetic Resonance technique called ‘inversion-recovery’ which can

not be explained here with a few words. Schubert *et al.* [11] used non-parametric background-characterization in the frequency domain.

C. Present Approach

In the present study, we address the problem by applying a State Space Approach devised by Kung *et al.* [13] and described in detail by Rao and Arun [14]. See also Ref. [15]. In MRS, the method is indicated by HSVD where H stands for a Hankel matrix formed from the sampled signal [12, 16]. HSVD models in terms of exponentially damped sinusoids and is used successfully for removing the signal of water molecules, omnipresent in living tissue. Note that water molecules are small and mobile; hence their spectrum is relatively narrow. In addition, its peak-frequency usually does not coincide with those of the tissue metabolites. Rather, the water spectrum buries the metabolite spectrum in its flanks. See *e.g.* [17, 18] for details about water- (or solvent-) suppression. The difference with macromolecule-suppression, addressed in the present study, is that the spectrum of macromolecules is broad and entirely overlaps that of the metabolites of interest.

D. Scope of Paper

This paper is set up as follows. Sec. II describes how we simulate a signal representing a background – or macromolecule – using analytical formulae. In Sec. III, we parameterize the background by means of HSVD (State Space approach), for various levels of added Gaussian noise. In Sec. IV, we superimpose a metabolite signal on the background signal. The sum is parameterized with HSVD, which enables subsequent separation of the two. The metabolite signal thus cleaned is finally quantitated with nonlinear least-squares model fitting. Conclusions are given in Sec. V.

II. BACKGROUND SIGNAL

A. Introduction

In this study, background signals are composed from four elementary shapes (≥ 0). Expressed in the frequency domain, these are 1) right-angled triangle, 2) rectangle, 3) the positive half of an ellipse, 4) one period of a cosine, augmented with unity. See Fig. 1. For presentation, the vertical scales have been adjusted such that the heights are equal. The angular frequency bounds ω_b of the shapes were chosen equal too, but in practice they are set independently, according to need.

Shifting of a shape over ω_s is done by multiplying the corresponding time domain signal by $\exp(i\omega_s t)$, where $i = \sqrt{-1}$. Broadening of a shape, in turn, is done by

multiplying in the corresponding time domain signal by *e.g.* $\exp[-\alpha t - (\beta t)^2]$ or some other damping function.

In practice, we normalize the area of a shape to

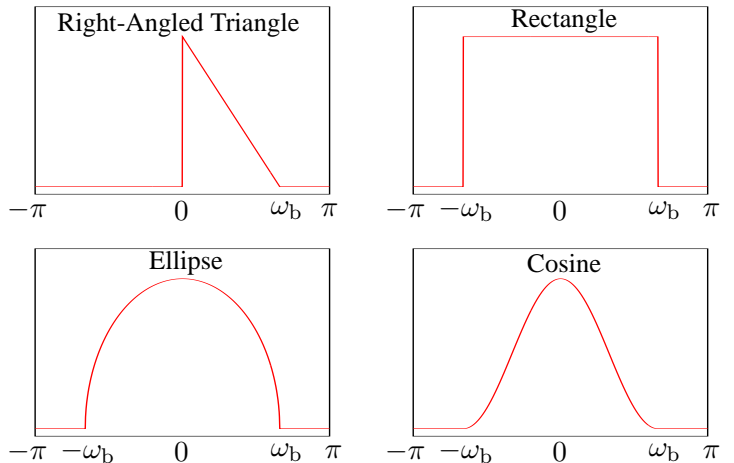


Fig. 1. Frequency-domain presentation of the four elementary shapes used for designing background spectra. Clock-wise, starting upper left: right-angled triangle, rectangle, ellipse, cosine. See also the formulae in the text. The triangle can be reflected with respect to $\omega = 0$ by changing the sign of ω_b .

unity. Consequently, the corresponding time-domain signal s_{shape} equals one at time $t = 0$, as follows from substituting the latter value in the Fourier transform formula [19].

$$s_{\text{shape}}(t) = \int_{-\infty}^{\infty} \text{shape}(\omega) e^{i\omega t} d\omega, \quad (1)$$

where the angular frequency ω equals 2π times the frequency ν .

For the sake of simplicity, only the signal for $t \geq 0$ is treated. In MR jargon, this assumption implies that one deals with so-called ‘free-induction decays’ or with the right-hand side of so-called ‘echoes’. Should one equate the signal for $t < 0$ to zero, then the spectral shapes would become complex-valued, as follows from the Fourier relation

$$\text{shape}(\omega) = \frac{1}{2\pi} \int_0^{\infty} s_{\text{shape}}(t) e^{-i\omega t} dt. \quad (2)$$

In the following sections, we consider only the real-valued parts of spectral shapes and ignore the signals for $t < 0$. This does not impair interpretation of the results.

Note our use of the continuous Fourier transform – Eqs. (1,2) – rather than its discrete approximation. This makes the relation between signal and spectrum exact and thus avoids a source of error in future comparisons of time and frequency domain procedures for background handling.

B. Right-angled Triangle

B.1 Frequency domain

For ω between 0 and ω_b , the spectral shape is

$$\text{triangle}(\omega_b, \omega) = \frac{2}{|\omega_b|} \left(1 - \frac{\omega}{\omega_b}\right), \quad (3)$$

and zero elsewhere. ω_b can be chosen between $-\pi$ and π .

B.2 Time domain

The corresponding signal s in the time domain is

$$s_{\text{triangle}}(\omega_b, t) = \frac{2}{(\omega_b t)^2} (1 + i\omega_b t - e^{i\omega_b t}). \quad (4)$$

C. Rectangle

C.1 Frequency domain

For $-\omega_b \leq \omega < \omega_b$, the spectral shape is

$$\text{rectangle}(\omega_b, \omega) = \frac{2}{\omega_b}, \quad (5)$$

and zero elsewhere, whereas $0 \leq \omega_b \leq \pi$.

C.2 Time domain

The corresponding signal s in the time domain is

$$s_{\text{rectangle}}(\omega_b, t) = \frac{\sin(\omega_b t)}{\omega_b t} \stackrel{\text{def}}{=} \text{sinc}(\omega_b t). \quad (6)$$

D. Ellipse

D.1 Frequency domain

For $-\omega_b \leq \omega < \omega_b$, the spectral shape is

$$\text{ellipse}(\omega_b, \omega) = \frac{2}{\omega_b \pi} \sqrt{1 - \frac{\omega^2}{\omega_b^2}}, \quad (7)$$

and zero elsewhere, whereas $0 \leq \omega_b \leq \pi$.

D.2 Time domain

The corresponding signal s in the time domain is

$$s_{\text{ellipse}}(\omega_b, t) = 2 \frac{J_1(\omega_b t)}{\omega_b t}. \quad (8)$$

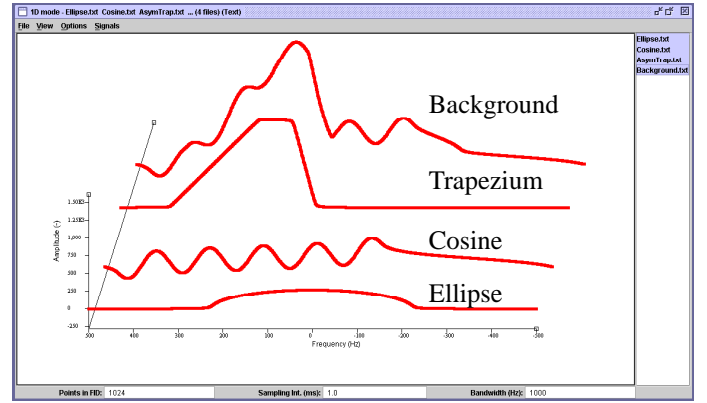


Fig. 2. Spectrum of a simulated macromole signal – background – using the four basic shapes shown in Fig. 1. First, a trapezium was made from a rectangle and two right-angled triangles. Next, an ellipse was added. Each was broadened and shifted by multiplication in the time domain with an appropriate exponential $\exp[-\alpha t - (\beta t)^2 + i\omega t]$. Finally, a series of five connected cosines was added to produce undulations. The phase of the cosines was rotated by 90 deg to augment the complexity.

E. Cosine

E.1 Frequency domain

For $-\omega_b \leq \omega < \omega_b$, the spectral shape is

$$\text{cosine}(\omega_b, \omega) = \frac{1}{2\omega_b} \left(1 + \cos\left(\frac{\omega}{\omega_b} t\right)\right), \quad (9)$$

and zero elsewhere, whereas $0 \leq \omega_b \leq \pi$.

E.2 Time domain

The corresponding signal s in the time domain is

$$s_{\text{cosine}}(\omega_b, t) = \text{sinc}(\omega_b t) + 0.5 \text{sinc}(\omega_b t + \pi) + 0.5 \text{sinc}(\omega_b t - \pi), \quad (10)$$

where the sinc function has been defined in Eq. (6).

F. Composition of a Background Signal

In this Section, we compose a background signal from the basic shapes introduced above. The background signal should be representative of a macromole signal. See [10] for examples of macromole signals of ^1H , and [9] for those of ^{31}P . The former possess more structure than the latter. This study aims at the former.

Although macromole signals may have many forms, we restrict ourselves to the one shown in Fig. 2. Its composition is described in the caption. In the frequency domain, it consists of two broad features – trapezium and ellipse – plus an undulating structure made up of five adjacent cosines. Spectral discontinuities have been removed by an extra multiplicative decay term in the time domain. Many alternative compositions are conceivable.

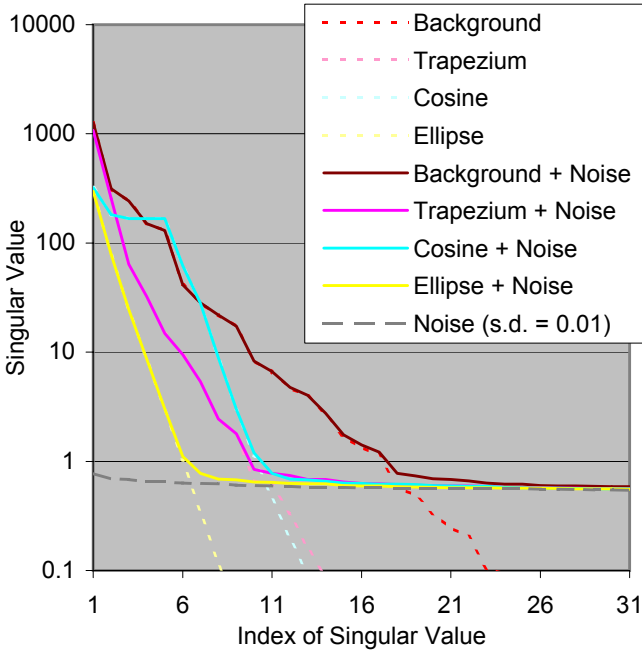


Fig. 3. Singular values of $L=512$ by $M=513$ Hankel matrices formed from the signals corresponding to the trapezium, ellipse, and cosine-series, and their sum, shown in Fig. 1, for one level of added noise. $N = 1024$.

III. PARAMETERIZATION OF BACKGROUND PLUS NOISE

A. State space modelling by HSVD

In HSVD, which is a State Space approach, the signal is modelled as a sum of exponentially damped sinusoids [12–16, 20]. The procedure is as follows. First, one forms an L by M Hankel matrix H from the time-domain signal s , sampled at regular intervals $t = n\Delta t$, with $n = 0, 1, \dots, N - 1$; $L \leq M$. When all samples are used, one has $L + M = N + 1$; depending on the signal-to-noise ratio, omitting the tail of the signal may be beneficial. Usually, H is chosen approximately square.

Next, H is subjected to Singular Value Decomposition (SVD)

$$H = U\Lambda V^\dagger, \quad (11)$$

where U is the left singular-vector matrix, Λ the diagonal singular-value matrix, V the right singular-vector matrix, and † denotes Hermitian conjugation. If the signal consists of K exactly exponentially damped sinusoids and is not corrupted by noise, then there are exactly K non-zero singular values $\lambda(k)$, $k = 1, 2, \dots, K$.

If the damping is non-exponential, as is the case for the signals given in Eqs. (4,6,8,10), then all singular values, $\lambda(k)$, $k = 1, 2, \dots, L$, are usually non-zero [15]. In other words, many exponentially damped sinusoids are needed to model a non-exponentially damped sinusoid. When

noise is added to the signal, all singular values become non-zero too. Examples of this are shown below.

As for the parameters of the exponentially damped sinusoids that model a signal $s(n)$, $n = 0, 1, \dots, N - 1$, according to

$$s(n) = \sum_{k=1}^{K_{\max}} c_k e^{[-\alpha_k + i\omega_k]n\Delta t + i\phi_k}, \quad (12)$$

HSVD first estimates the angular frequencies ω_k and exponential damping factors α_k from U , and subsequently estimates the amplitudes c_k and phases ϕ_k of the corresponding sinusoids by a linear least-squares fit to s [12–16, 20]. The maximum number of sinusoids K_{\max} deemed necessary for fitting is discussed in the next Subsection.

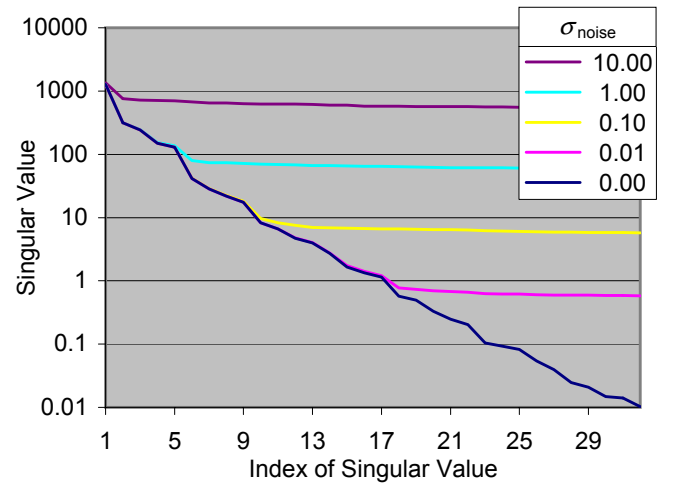


Fig. 4. Singular values of an $L=512$ by $M=513$ Hankel matrix formed from the signal corresponding to the background spectrum shown in Fig. 1, for five levels of added noise. $N = 1024$. Reduction of L and M by a factor of four, using only the first $L + M - 1$ samples, reduces the effect of noise significantly.

B. HSVD Modelling of a Background Signal

B.1 Preliminaries

Fig. 1 showed three individual shapes and the background composed from them. In this Subsection, we apply SVD to Hankel matrices formed from the corresponding signals with various amount of added Gaussian noise. Fig. 3 shows the singular values for the signals of the individual shapes and their sum, *i.e.* the background. The magnitudes of the signals at $t = 0$ are $|s(0)| = 200.01, 199.01, 499.2, 729.2$ (in arbitrary units) for trapezium, ellipse, cosine, and background, respectively.

It can be seen in Fig. 3 that each shape needs many singular values for proper modelling in terms exponentially damped sinusoids. The meaning of ‘proper’ is of course related to the noise level. To illustrate this, we plotted the

singular values of a Hankel matrix made up of Gaussian noise with standard deviation $\sigma_{\text{noise}} = 0.01$; see dashed line. If, at a certain index k , the singular value $\lambda(k)$ of the background signal drops below that dashed line, then at least k exponentially damped sinusoids are needed for modelling.

For further illustration, Fig. 4 shows the singular values of the background for five different levels of added Gaussian noise, and using all 1024 samples. It can be seen that at $\sigma_{\text{noise}} = 0.01$, at least 20 singular values would be needed for proper modelling, whereas at $\sigma_{\text{noise}} = 10$, this number drops to at least 5.

B.2 Optimal background modelling

As already said in Sec. I-A, the signal from a broad background decays fast and is therefore relatively short-lived. The number of samples used for modelling should be adapted accordingly. If too many samples are used, noise reduces the precision. Reduction of L and M by a factor of four, using only the first $L + M - 1$ samples, alleviates the effect of noise significantly. On the other hand, using too few samples limits the modelling space. Thus, the task is to find optimal values of the State Space (HSVD) parameters L , M , and K_{max} at a given noise level. In the present application, optimality pertains to *minimizing the error of metabolite quantitation* following subtraction of the parameterized background signal. The latter is addressed in the next Section.

IV. QUANTITATION OF SIGNALS SUPERIMPOSED ON BACKGROUND PLUS NOISE

A. Considerations

Once the background has been parameterized for certain values of L , M , and K_{max} , it can be subtracted from the signal. In view of unavoidable parameterization errors, the subtraction should be applied only to a minimal number of initial samples: There is no need to subtract background when its magnitude is smaller than the noise. On the other hand, if the background is not negligible with respect to the metabolite contribution to a sample, it should be subtracted.

Another aspect is how many and which of the K_{max} exponentially damped sinusoids to subtract. Subtraction of sinusoids with damping less than twice that of the metabolite components was avoided.

B. Results

The results obtained so far are compiled in Table I and Figs. 5, 6. For the sake of comparison, the simulated back-

ground was handled in four different ways: i) Background put to zero, no initial samples omitted. ii) Background put to zero, 45 initial samples omitted. iii) Non-zero background, handled by mere omission of 45 initial samples. iv) Non-zero background, 20 initial samples corrected by State Space approach HSVD.

In iv), we have investigated many values of the ‘procedure variables’ mentioned in Sec. IV-A. Here we present results for $L = 125$, $M = 126$, $K_{\text{max}} = 35$. All background components with damping ≤ 20 Hz – twice the damping value of the doublet components – were ignored; as a result, typically 13 to 23 of the $K_{\text{max}} = 35$ components were subtracted. See Fig. 5 for an example. The total number of samples in each signal was $N = 1024$.

Once the signal has been stripped of the background, the metabolites are quantified by the nonlinear least-squares time-domain fit programme AMARES [16]. See Table I. The true value of the estimated metabolite amplitudes is 5.0. All calculations were performed with the freely available *in vivo* MRS signal processing package jMRUI equipped with a Java-based graphical user interface [21].

Finally, all simulations were carried out for three noise levels, namely $\sigma_{\text{noise}} = 0.5, 1.0, 2.0$.

TABLE I

Results of a Monte Carlo experiment using 128 different noise realizations for each row of the Table. Averages of nonlinear least-squares time-domain estimates of metabolite signal amplitudes c_{-385} , c_{90} , c_{265} are given, along with their standard deviations σ_c , after handling of the background according to i, ii, iii, iv, described in Sec. IV-B. The true amplitudes are 5.0. See also graphical presentation in Fig. 6.

σ_{noise}	#	c_{-385}	σ_c	c_{90}	σ_c	c_{265}	σ_c
0.5	i	5.00	0.06	5.00	0.06	5.00	0.06
	ii	5.02	0.23	5.00	0.20	5.02	0.23
	iii	5.01	0.23	5.03	0.21	5.02	0.23
	iv	5.03	0.11	4.99	0.33	5.01	0.19
1.0	i	5.01	0.13	4.99	0.12	5.00	0.12
	ii	5.05	0.49	5.01	0.42	5.06	0.46
	iii	5.04	0.49	5.05	0.42	5.06	0.46
	iv	5.02	0.20	5.05	0.52	5.06	0.36
2.0	i	5.02	0.25	4.99	0.23	4.99	0.24
	ii	5.21	1.23	5.09	0.86	5.19	0.98
	iii	5.21	1.23	5.12	0.87	5.19	0.98
	iv	5.05	0.40	4.98	1.13	5.31	0.87

C. Discussion

Judging from Fig. 5, background parameterization and subsequent subtraction without using prior knowledge works well. Table I, rows iii and iv for each σ_{noise} , reveals

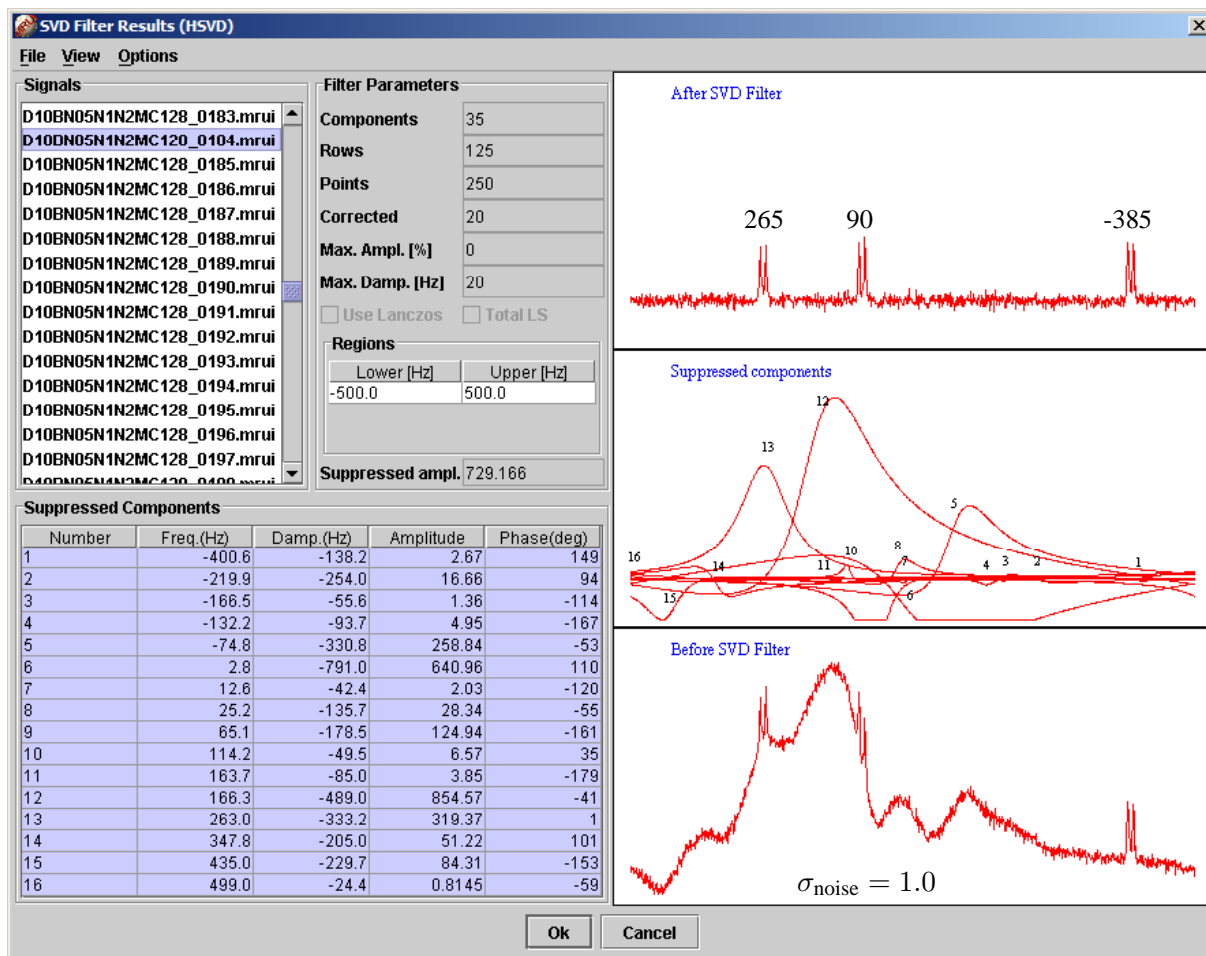


Fig. 5. Background removal by HSVD. Bottom-right: Three metabolite doublets superimposed on the broad background shown in Fig. 2. Middle-right: HSVD-parameterized background comprising 16 components. Upper-right: Difference between the previous two, showing clearly the three metabolite doublets, at 265 Hz, 90 Hz, and -385 Hz. The amplitudes and damping factors of all doublet components are 5.0 (in arbitrary units) and 10 Hz, respectively.

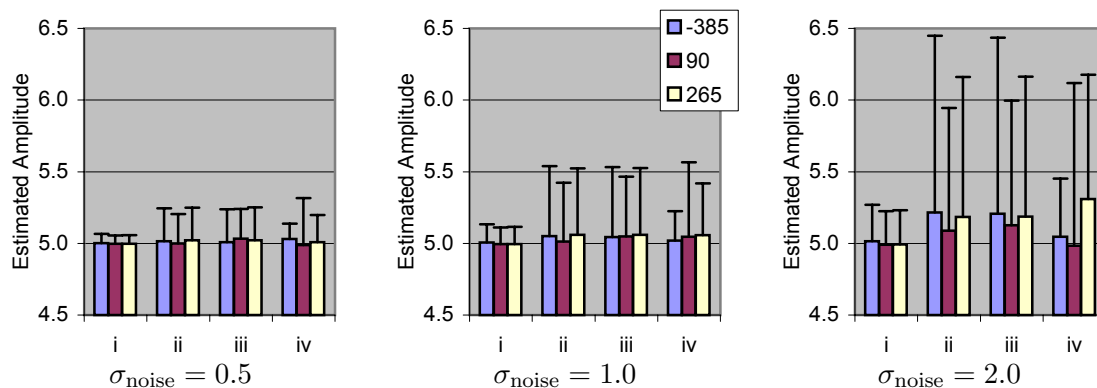


Fig. 6. Graphical presentation of the results in Table I.

that the trade-off between bias and standard deviation can yet be improved. This is important because *in vivo* MRS usually offers time for only one measurement. Rows i and ii pertain to absence of background and therefore yield def-

inite lower bounds on the overall error.

Study of the Cramér-Rao lower bounds (CRB's), including background estimation, for rows iv of Table I is highly desirable [7]. But in absence of the true background model

function – for *in vivo* MRS – this seems impossible. As substitute, we plan calculation of the CRB’s using background modelling as shown in Fig. 5, along the lines of Ref. [20].

V. CONCLUDING REMARKS

- The State Space approach HSVD automatically parameterizes complicated background signals. Fine-tuning is yet to be finalized.
- Subtraction of a parameterized background signal salvages the metabolite contribution to the initial samples. This improves the quantitation of metabolites.
- In some cases, mere omission of initial samples yields equally good quantitation of metabolites.
- We derived formulae for realistic, non-exponentially damped, *in vivo* MRS background signals. Their exact continuous Fourier transforms are given for future comparison of time- and frequency-domain background-handling methods.

ACKNOWLEDGMENTS

This work is supported by the Dutch Technology Foundation STW and the EU TMR/Networks Project ERB-FMRX-CT97-0160.

REFERENCES

- [1] I.C.P. Smith and L.C. Stewart, “Magnetic resonance spectroscopy in medicine: clinical impact,” *Progress in Nuclear Magnetic Resonance Spectroscopy*, vol. 40, pp. 1–34, 2002.
- [2] A. van den Bos, *Parameter Estimation*, chapter 8, John Wiley and Sons, 1982, In: Handbook of Measurement Science, Vol. 1, P.H. Sydenham Ed.
- [3] J. Higinbotham and I. Marshall, “NMR Lineshapes and Lineshape Fitting,” *Annual Reports on NMR Spectroscopy*, vol. 43, pp. 59–120, 2001.
- [4] V. Govindaraju, K. Young, and A.A. Maudsley, “Proton NMR chemical shifts and coupling constants for brain metabolites,” *NMR in Biomedicine*, vol. 13, pp. 129–153, 2000.
- [5] S.W. Provencher, “Automatic quantitation of localized *in vivo* H-1 spectra with LCMODEL,” *NMR in Biomedicine*, vol. 14, pp. 260–264, 2001.
- [6] P.H. Hodgkinson and P.J. Hore, “Sampling and the quantification of NMR data,” *Advances in Magnetic and Optical Resonance*, vol. 20, pp. 187–244, 1997.
- [7] S. Cavassila, S. Deval, C. Huegen, D. van Ormondt, and D. Graveron-Demilly, “Cramér-Rao bound expressions for parametric estimation of overlapping peaks. Influence of prior knowledge,” 2000.
- [8] S. Cavassila, S. Deval, C. Huegen, D. van Ormondt, and D. Graveron-Demilly, “Cramér-Rao bounds: A tool for quantitation objectives,” *NMR in Biomedicine*, vol. 14, pp. 278–283, 2001.
- [9] J.A. Stanley and J.W. Pettegrew, “Postprocessing method to segregate and quantify the broad components underlying the phosphodiester spectral region of *in vivo* ³¹P brain spectra,” *Magnetic Resonance in Medicine*, vol. 45, pp. 390–396, 2001.
- [10] U. Seeger, I. Mader, T. Nägele, W. Grodd, O. Lutz, and U. Klose, “Reliable detection of macromolecules in single volume 1H NMR spectra of the human brain,” *Magnetic Resonance in Medicine*, vol. 45, pp. 948–954, 2001.
- [11] F. Schubert, F. Seifert, C. Elster, A. Link, M. Walzel, S. Mientusand, J. Haas, and H. Rinneberg, “Serial 1H-MRS in relapsing-remitting multiple sclerosis: effects of interferon-beta therapy on absolute metabolite concentrations,” *Magnetic Resonance Materials in Physics Biology and Medicine*, vol. 14, pp. 213–222, 2002.
- [12] R. de Beer and D. van Ormondt, “Analysis of NMR data using time domain fitting,” in *NMR Basic Principles and Progress*, P. Diehl, E. Fluck, H. Gunther, R. Kosfeld, and J. Seelig, Eds., pp. 202–248. Springer-Verlag, Berlin, 1992.
- [13] S.Y. Kung, K.S. Arun, and B.D. Rao, “State-space singular value decomposition based methods for the harmonic retrieval problem,” *Journal of the Optical Society of America*, vol. 73, pp. 1799–1811, 1983.
- [14] B.D. Rao and K.S. Arun, “Model-Based Processing of Signals: A State Space Approach,” *Proc IEEE*, vol. 80, pp. 283–309, 1992.
- [15] R. de Beer, D. van Ormondt, S. Cavassila, D. Graveron-Demilly, and S. Van Huffel, “SVD-based Modelling of Medical NMR signals,” in *SVD and Signal Processing III*, M. Moonen and B. de Moor, Eds. 1994, pp. 467–474, Elsevier.
- [16] L. Vanhamme, T. Sundin, S. Van Huffel, and P. Van Hecke, “Spectroscopic MRS Data Quantitation: A Review of Time Domain Methods,” *NMR in Biomedicine*, vol. 14, pp. 233–246, 2001.
- [17] J.W.C. van der Veen, D.R. Weinberger, G. Tedeschi, J.A. Frank, and J.H. Duyn, “Proton Spectroscopic Imaging without Water Suppression,” *Radiology*, vol. 217, pp. 296–300, 2000.
- [18] A. Coron, L. Vanhamme, J-P. Antoine, P. Van Hecke, and S. Van Huffel, “The filtering approach to solvent peak suppression in MRS: a critical review,” *Journal of Magnetic Resonance*, vol. 152, pp. 26–40, 2001.
- [19] R.N. Bracewell, *The Fourier Transform and its Applications*, McGraw-Hill, 1978.
- [20] S. Cavassila, A. Briguet, D. Graveron-Demilly, C. Decanniere, P. Van Hecke, S. Van Huffel, and D. van Ormondt, “Quantification of nondescript peaks with SVD-based methods and estimation of errors,” in *Society of Magnetic Resonance*, San Francisco, 1994, p. 1187.
- [21] “<http://www.mrui.uab.es/mrui/mruiHomePage.html>,” .